

OR3-7

高融点単原子液体の構造と物性

Structure and Properties of monatomic liquids with high melting temperature

水野章敏^{1,5}、寺門修¹、鎌田アハメッド¹、中野彩花¹、尾原幸治²、正木匡彦³、渡邊学⁴、小原真司⁵
Akitoshi MIZUNO^{1,5}, Osamu TERAKADO¹, Ahmed KAMADA¹, Ayaka NAKANO¹, Koji OHARA²,
Tadahiko MASAKI³, Manabu WATANABE⁴ and Shinji KOHARA⁵

¹函館工業高等専門学校, National Institute of Technology (KOSEN), Hakodate College,

²島根大学, Shimane University,

³芝浦工業大学, Shibaura Institute of Technology,

⁴東京工業大学, Tokyo Institute of Technology,

⁵物質・材料研究機構, National Institute for Materials Science

1. Introduction

In recent years, machine learning using liquid metal properties and theoretical models as input has led to rapid progress in the development of metallic glasses as well as many functional materials¹⁻³. For liquid and amorphous metal oxides, a study was reported that use their liquid and amorphous structure data as input for machine learning, which was applied to optimize model potentials and predict chemically realistic structures⁴. It is therefore expected to become important in the future to use liquid structures as training data for machine learning to predict glass-forming ability of metallic alloys. However, as metallic glasses are often multicomponent alloys, it takes a lot of time to cover their liquid structures because of numerous experimental conditions with different combinations of composition and temperature. Hence, it is important to predict the liquid structure of alloys from monatomic liquid structures.

Recent advances in containerless techniques have made it possible to perform experimental studies of properties and structure of elemental liquids with high melting temperature. Many experimental data on thermophysical properties such as density, viscosity and surface tension have been obtained by electrostatic levitation on the ground and under microgravity conditions^{5,6}. Although fewer in number than the thermophysical properties, experimental data on the structure of metallic liquids have been systematically compiled⁷ and recently obtained by combining synchrotron radiation X-ray diffraction (SR-XRD) with levitation techniques including aerodynamic levitation (ADL)⁸. However, there are very few reports on elements with melting temperature above 2500 K.

The aim of this study was to systematize liquid structure information by focusing on the main constituent elements of metallic glasses and performing precise structure analysis of metallic liquids at high temperature typically over 2000 K. In the present study, structural data for eight elements, including Hf with a melting point of 2506 K, were measured using a combination of the SR-XRD and the ADL technique. In addition, persistent homology (PH) analysis^{9,10} was performed on 3D coordinates obtained from reverse Monte Carlo (RMC)

modelling¹¹⁾ to reproduce the measured structure data, and relationships with thermophysical property such as entropy were investigated.

2. Experimental

2.1. Aerodynamic levitation (ADL) furnace for synchrotron radiation X-ray diffraction (SR-XRD)

As the details of the experimental setup are similar to those in previous papers^{12,13)}, only a brief summary is described in this paper. To obtain the X-ray scattering data of chemically active liquids at high temperatures, the ADL furnace was used as shown in Fig. 1. A conical nozzle was installed in a high vacuum chamber filled with high-purity Ar gas. A spherical sample of approximately 2 mm diameter was levitated in the nozzle by controlling the gas flow rate with a mass flow controller. A CO₂ laser with a maximum power of 200 W (Synrad, firester f200) was used to melt the sample and the temperature of the sample was monitored using a two-color optical pyrometer (Impac, ISR 12-LO).

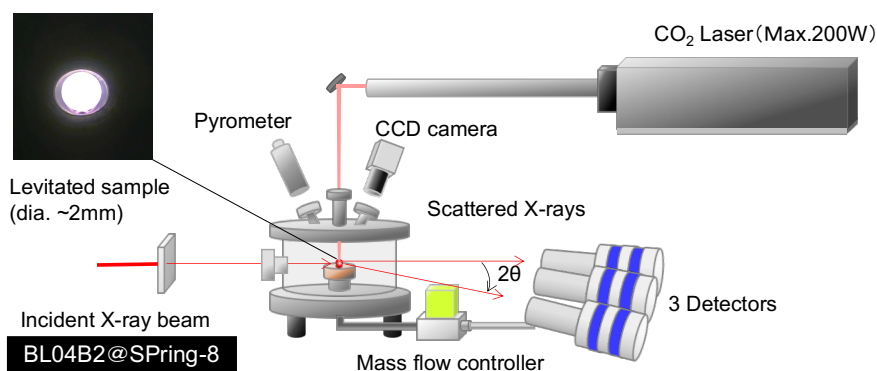


Figure 1. Schematic diagram of the aerodynamic levitation apparatus constructed for synchrotron x-ray diffraction (SR-XRD) experiments.

The SR-XRD experiments were carried out at the BL04B2 and BL08W beamlines of SPring-8. The experimental conditions were optimized at the BL08W beamline, and the experiments were conducted under optimum conditions at the BL04B2 beamline. Monochromatic X-rays with an energy of 112.7 keV were irradiated into the sample and the scattered X-rays were detected by three Ge Solid state detectors (SSD) with the scattering angle, 2θ , ranging from 0.3° to 25° . To confirm the reproducibility of the scattering intensity, the measurement was repeated three or more times in the same angular range per sample. The temperature conditions were just above the melting temperature of the measured element, including the supercooled liquid state. The liquid static structure factor, $S(Q)$, was extracted from the scattering intensity through the usual corrections as a function of the scattering vector magnitude $Q (=4\pi\sin\theta/\lambda$, where λ is the wavelength of the incident X-ray).

2.2. Liquid structure analysis

Since the $S(Q)$ is information in reciprocal space, it can be analyzed as information in real space by estimating the pair distribution function (PDF), $g(r)$, by the following Fourier transform relation:

$$g(r)-1 = \frac{1}{2\pi^2 \rho_0 r} \int_{Q_{\min}}^{Q_{\max}} Q(S(Q)-1) \sin QrdQ , \quad (1)$$

where ρ_0 is the average number density. As the PDF represents the three-dimensional atomic arrangement as a one-dimensional distribution, the structural information obtained is limited to the distance between nearest neighbor atoms and the coordination number. Therefore, the RMC method¹¹⁾ was used to reproduce the three-dimensional atomic coordinates based on the $S(Q)$ obtained from experiments. In the present study, the RMC was performed for 10000 particles in a cubic box to reproduce the $S(Q)$ obtained from the SR-XRD experiments. The volume of the cubic box was estimated from the experimental density¹⁴⁾.

2.3. Persistent homology (PH) analysis

In recent years, PH analysis, one of the topological data analysis methods, has been developed as a structure analysis method for amorphous materials and glasses^{9,10)}. PH analysis can be applied to atomic arrangements obtained by the RMC method to extract and visualize hierarchical structures. As shown in Fig. 2, the radius of an atom in 3D coordinates is simultaneously increased, and the radius when a ring (hole) appears after overlapping with neighboring atoms is assigned as “birth” time, and the radius when the ring disappears after further increase is assigned as “death” time. A persistent diagram (PD), with the radius at “birth” time on the horizontal axis and the radius at “death” time on the vertical axis, allows the extraction of crystalline, liquid and glassy structural features from the distribution⁹⁾.

The main feature of this method is that it can analyze the shape of voids (homology) without defining the bonds between atoms, thus eliminating the problem of selecting the cut-off range of interest in structure analysis, such as Voronoi polyhedral analysis. In this study, the HomCloud package¹⁰⁾, an application for PH analysis, was used.

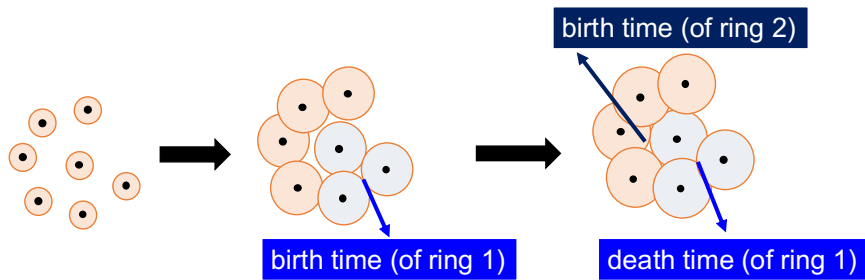


Figure 2. Schematic illustration showing the rings on birth time and death time defined in the Persistent Homology (PH) analysis.

2.4. Configuration entropy

The relationship between the structure and physical properties of liquids has long been a topic of experimental and theoretical research, and in particular, the following relationship have been proposed for the PDF, $g(r)$, and entropy S :

$$S = S^{(1)} + S^{(2)} + S^{(3)} + \dots, \quad (2)$$

$$S^{(2)} = -2\pi\rho_0 \int \{g(r) \ln g(r) - [g(r) - 1]\} r^2 dr, \quad (3)$$

where $S^{(1)}$, $S^{(2)}$ and $S^{(3)}$ represent the entropy due to ideal gas, two-body (pair) and three-body (triplet) correlations, respectively, and the table equation takes many-body correlations into account^{15,16}. However, it is difficult to obtain correlations for more than three bodies, and many approximate models have been proposed. In the present study, since the focus is on pair correlations, the two-body term $S^{(2)}$ was calculated using the PDF $g(r)$ estimated from the experimental $S(Q)$.

3. Results and Discussion

3.1. Liquid structure factor $S(Q)$

The elements for which liquid $S(Q)$ s were successfully obtained in this study are shown in Fig. 3. As the main components of metallic glasses are mostly transition elements framed in the figure, measurements were also carried out on Si, a high-melting metalloid, as a comparison. The elements for which liquid $S(Q)$ could not be obtained in the present study were due to insufficient laser power (maximum power: 200 W) or the low absorption rate of the CO₂ laser (laser emission wavelength: 10.6 μm). Therefore, it is necessary to use a laser with even higher power or a semiconductor laser with emission wavelengths that are highly absorbed by metallic elements.

	1	2	3	4	5	6	7	8	9	10	11	12	13	14	15	16	17	18
1																		
2			Melting temperature: unit in Kelvin															
3			Hatched elements: Measured in the present study															
4																		
5																		
6																		
7																		

21Sc	22Ti	23V	24Cr	25Mn	26Fe	27Co	28Ni	29Cu
1814	1941	2183	2180	1519	1811	1768	1728	1358
39Y	40Zr	41Nb	42Mo	43Tc	44Ru	45Rh	46Pd	47Ag
1799	2128	2750	2896	2430	2607	2237	1829	1235
57-71	72Hf	73Ta	74W	75Re	76Os	77Ir	78Pt	79Au
	2506	3290	3695	3459	3306	2739	2041	1337

14Si	1685
------	------

Figure 3. Elements for which liquid $S(Q)$ was measured in the present study.

The representatives of measured $S(Q)$ of the monatomic liquids in comparison with the RMC results of $S(Q)$ and the corresponding PDF, $g(r)$, are shown in Fig. 4. The use of three detectors enabled SR-XRD data to be acquired in a shorter time than in the past experiments, and $S(Q)$ could be obtained over a wide Q range. For the transition elements, an asymmetric shape, called a “shoulder”, is observed on the high Q side of the second peak of $S(Q)$ around 50 nm^{-1} . On the other hand, for liquid Si, a shoulder is observed more clearly on the high Q side of the first peak of $S(Q)$ around 35 nm^{-1} . This feature of the $S(Q)$ of liquid Si is thought to be related to its covalent nature.

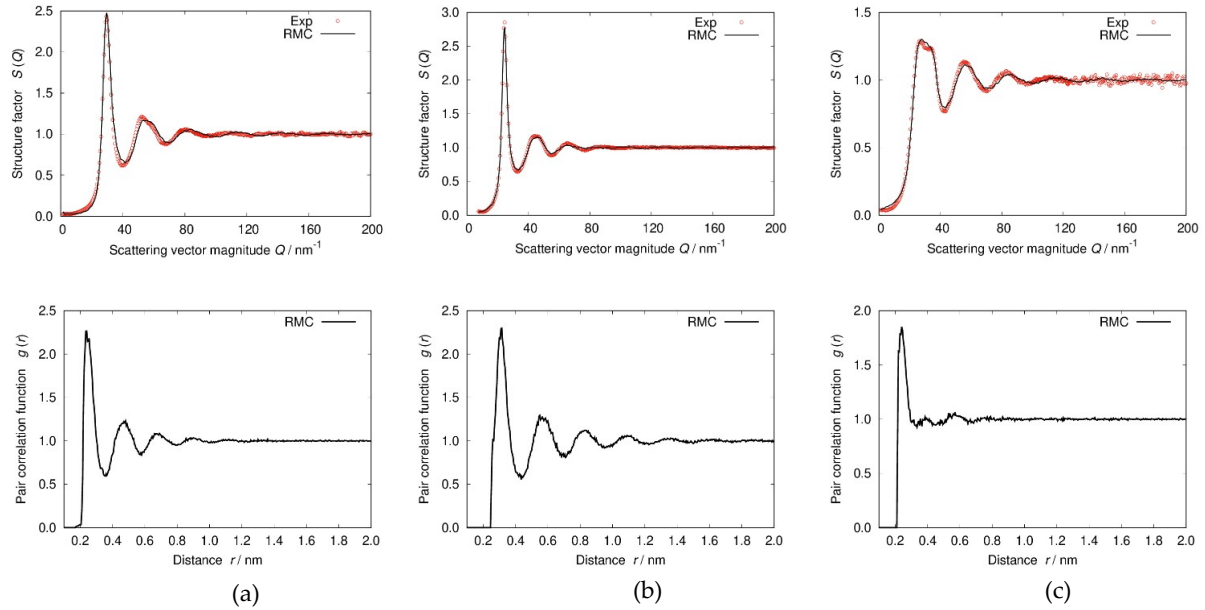


Figure 4. Comparison of experimental liquid $S(Q)$ with RMC results and corresponding PDF $g(r)$ for (a) Fe at 1820 K (T_m : 1811 K), (b) Hf at 2510 K (T_m : 2506 K), (c) Si at 1700 K (T_m : 1685 K).

As shown in the upper part of Fig. 5, the distribution of free volume around each atom can be visualised for the 3D coordinates of the atomic configuration obtained by the RMC method. The free volume distribution of Si is considerably more spread out than that of Fe and Hf, indicating that the structure of the Si liquid is sparse, whereas the Fe and Hf liquids are closer to a densely packed structure.

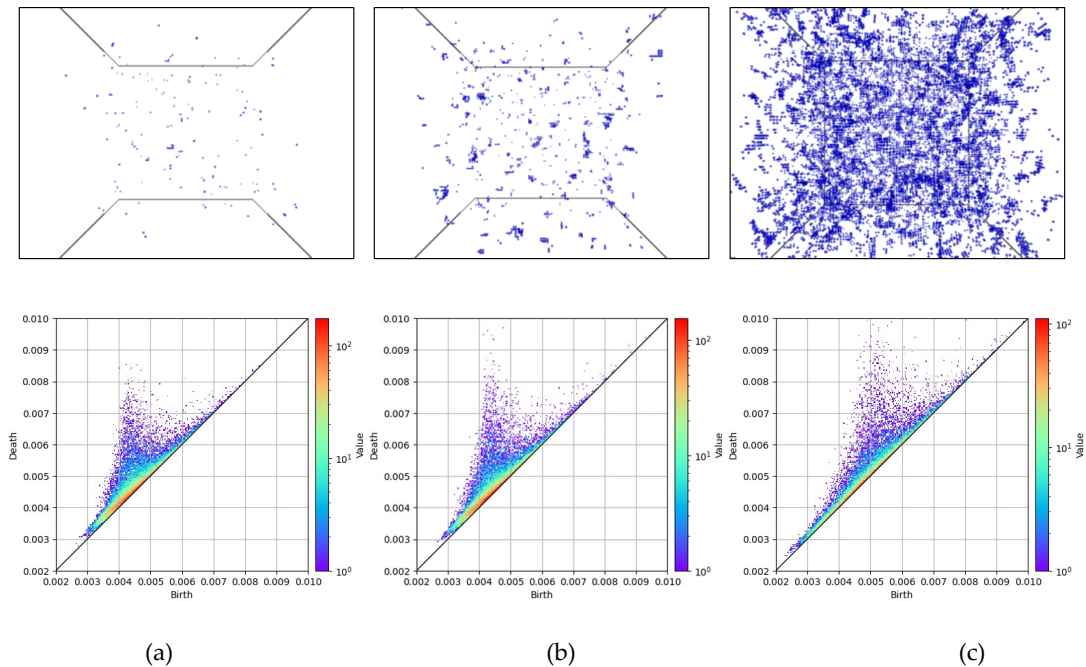


Figure 5. Comparison of free volume distributions (upper side) and PD2 (lower side) obtained from 3D coordinates by RMC modelling for liquid $S(Q)$, for (a) Fe at 1820 K (T_m : 1811 K), (b) Hf at 2510 K (T_m : 2506 K), (c) Si at 1700 K (T_m : 1685 K).

The results of the PH analysis of the atomic configurations obtained by the RMC method are also shown in lower part of Fig. 5 as two-dimensional PD (PD2), which can be considered to represent the distribution of the radii of formation and annihilation of voids (free volume). The values of Birth and Death radii of the

annihilation of voids are not widely scattered from the PD of Fe and Hf. On the other hand, the values of both Birth and Death radii for Si are widely distributed up to large values. Therefore, it can be interpreted that the voids in the atomic configuration are large and widely distributed. This is consistent with the results for the distribution of free volumes presented in the upper part of Fig. 5, indicating that PH analysis is effective in capturing the feature of atomic-scale packing in liquids.

To obtain more insight into the relationship between the results of the structural analysis and the thermophysical properties, the entropy $S^{(2)}$ of the two-body correlation calculated from the PDF are shown in Fig. 6. In the present study, due to the small number of data points and the narrow temperature range, the temperature dependence was approximated as a linear equation. Equations (2) and (3) represent that for the two-body term $S^{(2)}$, the smaller its value, the smaller the total entropy S . Therefore, the temperature dependence shows a reasonable trend. In addition, transition metals have a smaller $S^{(2)}$, which suggests that they have more ordered liquid structures than Si.

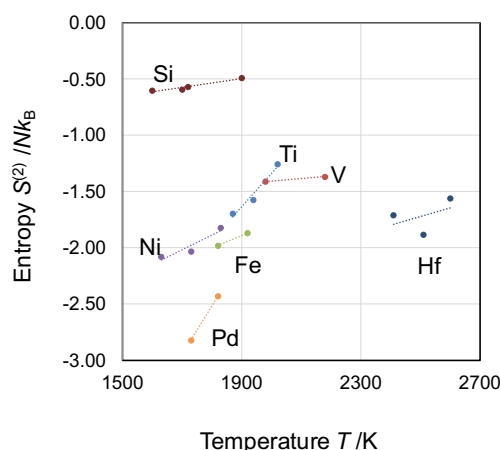


Figure 6. Temperature dependence of the entropy $S^{(2)}$ of the two-body correlation calculated from the PDF.

4. Conclusion

In the present study, liquid structure factors $S(Q)$ s for eight elements, including Hf with a melting point of 2506 K, were measured using a combination of ADL and SR-XRD. PH analysis was performed on 3D coordinates obtained from RMC modelling to reproduce the obtained $S(Q)$. The PH analysis and the free volume distribution estimated from the RMC results indicate a dense liquid structure of transition metals and a sparse liquid structure of Si. Furthermore, it was shown to be qualitatively related to macroscopic thermophysical properties such as entropy calculated from the PDF.

Acknowledgement

This work was supported by JSPS KAKENHI (Grant Number JP 20H02496, 23K04464) and the synchrotron radiation experiments were performed at the BL08W and the BL04B2 of SPring-8 with the approval of the Japan Synchrotron Radiation Research Institute (JASRI) (Proposal No. 2021A1445, No. 2021B1280).

References

- 1) L. Ward, S.C. O'Keefe, J. Stevick, G. R. Jelbert, M. Aykol, C. Wolverton: A machine learning approach for engineering bulk metallic glass alloys. *Acta Mater.*, **159** (2018) 102. DOI: 10.1016/j.actamat.2018.08.002.

- 2) F. Ren, L. Ward, T. Williams, K.J. Laws, C. Wolverton, J. Hatrick-Simpers, A. Mehta: Accelerated discovery of metallic glasses through iteration of machine learning and high-throughput experiments. *Sci. Adv.*, **4** (2018), 1566, DOI: 10.1126/sciadv.aaq1566.
- 3) A. Ghorbani, A. Askari, M. Malekan, M. Nili-Ahmadabadi: Thermodynamically guided machine learning modelling for predicting the glass-forming ability of bulk metallic glasses. *Sci. Rep.*, **12** (2022), 11754, DOI: 10.1038/s41598-022-15981-2.
- 4) G. Sivaraman, G. Csanyi, A. Vazquez-Mayagoitia, I. T. Foster, S. K. Wilke, R. Weber, C. J. Benmore: A Combined Machine Learning and High-Energy X-ray Diffraction Approach to Understanding Liquid and Amorphous Metal Oxides. *J. Phys. Soc. Jpn.*, **91** (2022) 091009, DOI: 10.7566/JPSJ.91.091009.
- 5) T. Ishikawa, J. T. Okada, P. F. Paradis, Y. Watanabe: Thermophysical property measurements of high temperature melts using an electrostatic levitation method. *Jpn. J. Appl. Phys.*, **50** (2011) 11RD03. DOI: 10.1143/JJAP.50.11RD03.
- 6) P.-F. Paradis, T. Ishikawa, G.-W. Lee, D. Holland-Moritz, J. Brillo, W.-K. Rhim, J. T. Okada: Materials properties measurements and particle beam interactions studies using electrostatic levitation. *Mater. Sci. Eng. R Rep.*, **76** (2014) 1, DOI: 10.1016/j.mser.2013.12.001.
- 7) Y. Waseda: *The Structure of Non-Crystalline Materials : Liquids and Amorphous Solids*, McGraw-Hill (1980).
- 8) S. Krishnan and D. L. Price: X-ray diffraction from levitated liquids. *J. Phys. Condens. Matter*, **12** (2001) R145, DOI: 10.1088/0953-8984/12/12/201.
- 9) Y. Hiraoka, T. Nakamura, A. Hirata, E.G. Escobar, K. Matsue, Y. Nishiura: Hierarchical structures of amorphous solids characterized by persistent homology. *Proc. Natl. Acad. Sci. USA*, **113** (2016) 7035, DOI: 10.1073/pnas.1520877113.
- 10) I. Obayashi, T. Nakamura, Y. Hiraoka: Persistent Homology Analysis for Materials Research and Persistent Homology Software: HomCloud. *J. Phys. Soc. Jpn.*, **91** (2022) 091013, DOI: 10.7566/JPSJ.91.091013.
- 11) R. L. McGreevy and L. Pusztai: Reverse Monte Carlo Simulation: A New Technique for the Determination of Disordered Structures. *Molec. Simul.*, **1** (1988) 359, DOI: 10.1080/08927028808080958.
- 12) A. Mizuno, S. Matsumura, M. Watanabe, S. Kohara, M. Takata: High-energy x-ray diffraction study of liquid structure of metallic glass-forming $Zr_{70}Cu_{30}$ Alloy. *Mater. Trans.*, **46** (2005) 2799, DOI: 10.2320/matertrans.46.2799.
- 13) A. Mizuno, H. Oka, T. Akimoto, Y. Yokoyama, M. Itou, S. Kohara, M. Watanabe : Time-Resolved X-ray Diffraction during Container less Solidification of Zr-Based Alloys.(in Japanese) *J. Jpn. Soc. Microgravity*, **27** (2010) 222, DOI: 10.15011/jasma.27.4.222.
- 14) Y. Marcus: On the compressibility of liquid metals. *J. Chem. Thermodyn.*, **109** (2017) 11, DOI: 10.1016/j.jct.2016.07.027.
- 15) A. Baranyai and D. J. Evans: Direct entropy calculation from computer simulation of liquids. *Phys. Rev. A*, **40** (1989) 3817, DOI: 10.1103/PhysRevA.40.3817.
- 16) Jakse, N., Pasturel: Excess Entropy Scaling Law for Diffusivity in Liquid Metals. *Sci. Rep.*, **6** (2016) 20689, DOI: 10.1038/srep20689.



© 2023 by the authors. Submitted for possible open access publication under the terms and conditions of the Creative Commons Attribution (CC BY) license (<http://creativecommons.org/licenses/by/4.0/>).